Supporting Information

Introducing Ti^{3+} Defects Based on Lattice Distortion for Enhanced Visible Light Photoreactivity in TiO_2 Microspheres

Yunfan Xu [a,b] Sujuan Wu [a*] Piaopiao Wan [a] and Jianguo Sun [a] and Zachary D. Hood[c,d]

[a.] Electron Microscopy Center of Chongqing University, College of Materials Science and Engineering, Chongqing University, Chongqing, China.
[b.] Laboratory of Advanced Materials, Department of Materials Science and Engineering, Tsinghua University, Beijing, China.
[c.] School of Chemistry and Biochemistry, Georgia Institute of Technology, Atlanta, Georgia 30332, United States
[d.] Center for Nanophase Materials Sciences, Oak Ridge National Laboratory, Oak Ridge, Tennessee 37831, United States

Corresponding Author：Sujuan Wu
Email: sujuan.wu@cqu.edu.cn

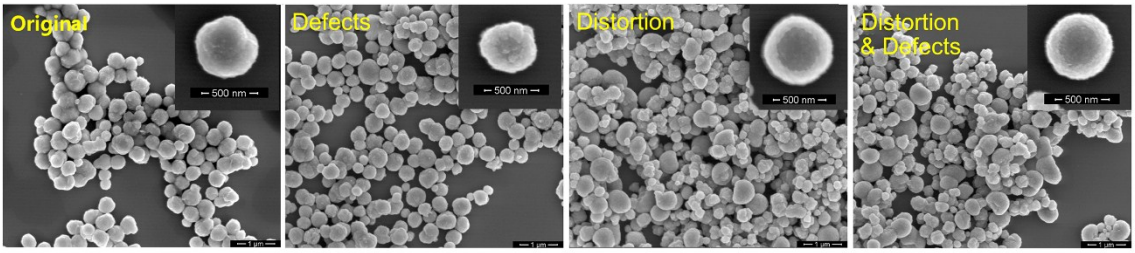

Figure S1. SEM images of as-prepared TiO_2 samples. The morphology of as-prepared TiO_2 samples greatly change when chloride ions are added.

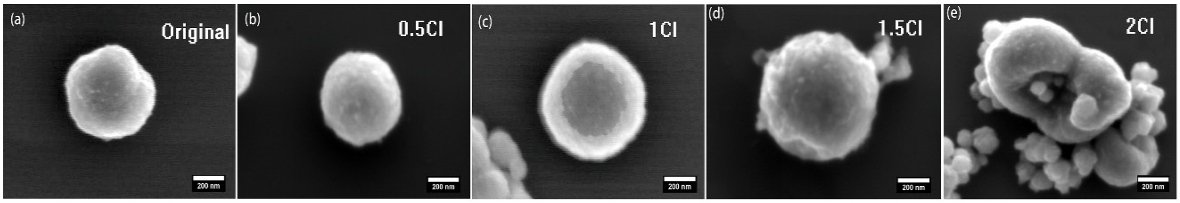

Figure S2. SEM images of as-prepared TiO_2 samples of different chloride ion content (noted on the images). It can be inferred that the chloride ions acts as surface surfactant.

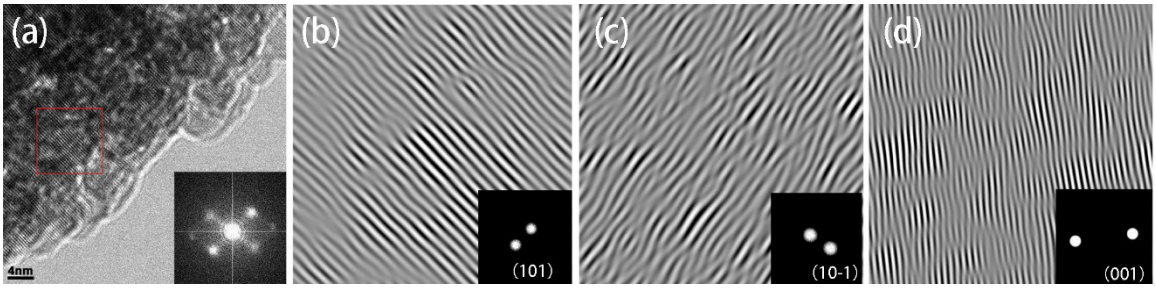

Figure S3. FFT of the lattice distorted TiO_2 sample. Great lattice distortions can be observed.

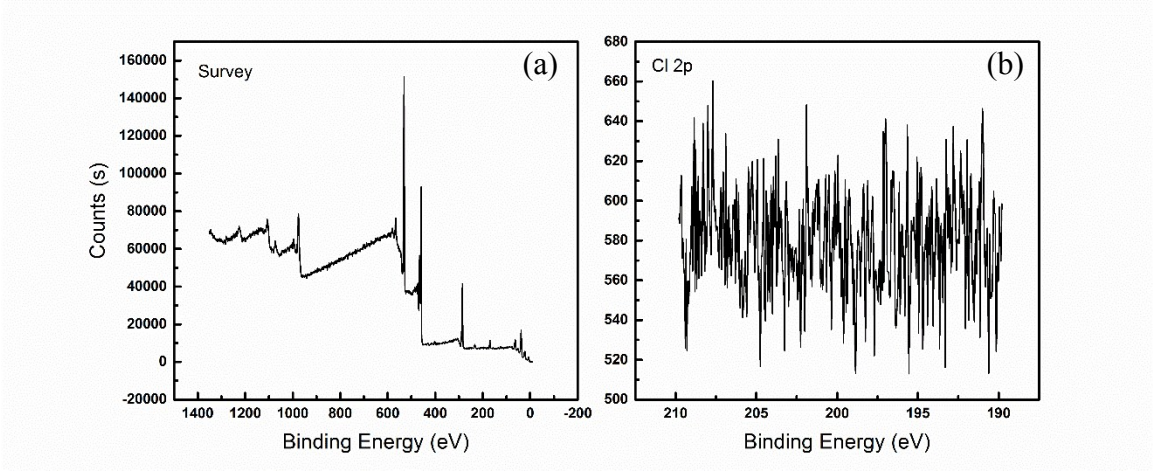

Figure S4. (a) XPS survey spectrum of lattice distorted TiO_2; (b) Cl 2p XPS spectrum of TiO_2 with lattice distortion.

No chlorine signal was present in the high resolution Cl 2p scan.

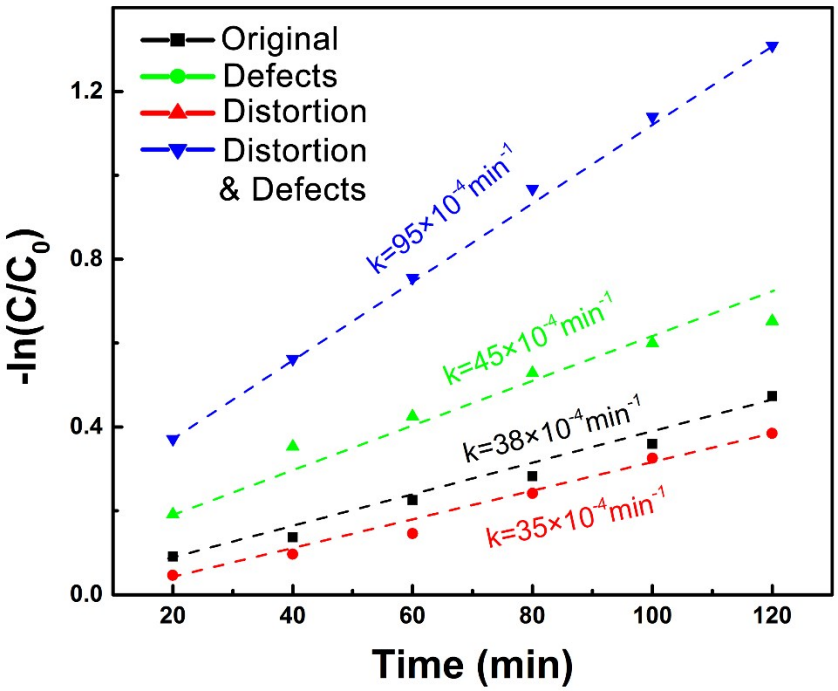

Figure S5. Kinetic fit for the degradation of RhB under visible light irradiation. The TiO_2 hollow microspheres with both lattice distortion and Ti^{3+} defects achieved the highest degradation rate of RhB under visible light irradiation.

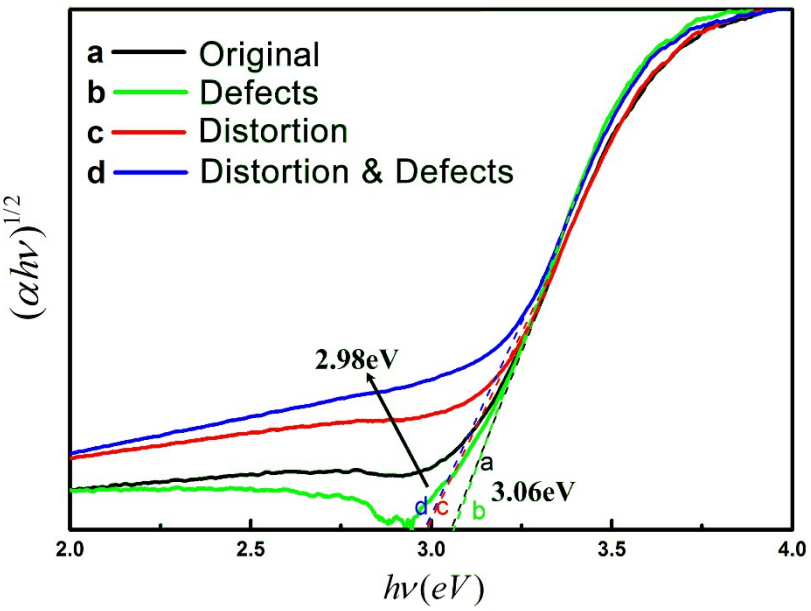

Figure S6. $(\Box E_{photon})^{1/2}$ vs E_{photon} curves of TiO_2 microspheres. The band gap of Original, Defects, Distortion, and Distortion & Defects are 3.06 eV, 2.98 eV, 3.06 eV, and 2.98 eV, respectively.

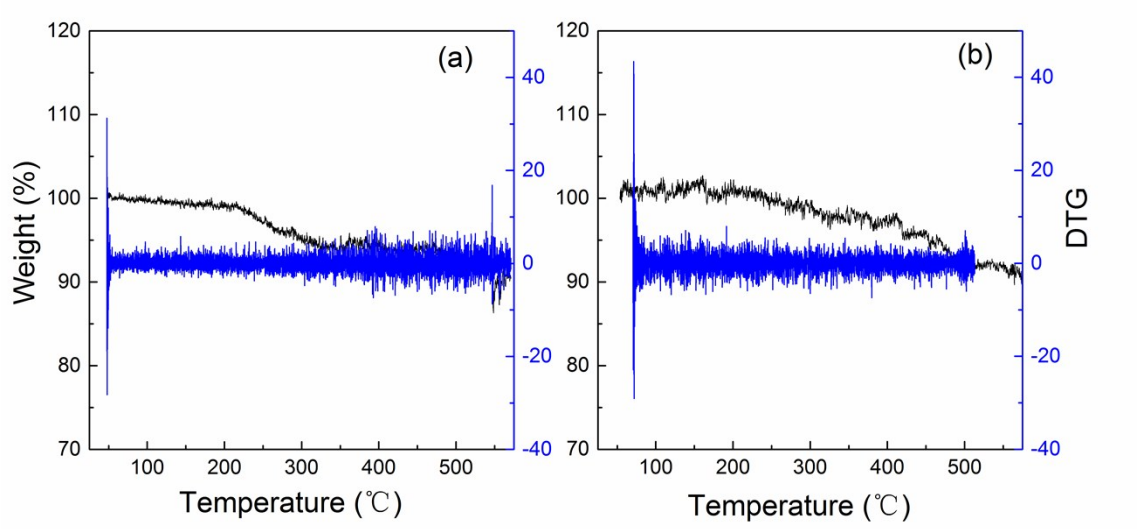

Figure S7.TG and DTG curves of (a) Defects and (b) Distortion & Defects.
It can be seen from the TGA curves that no organic matter remains after EG reduction.

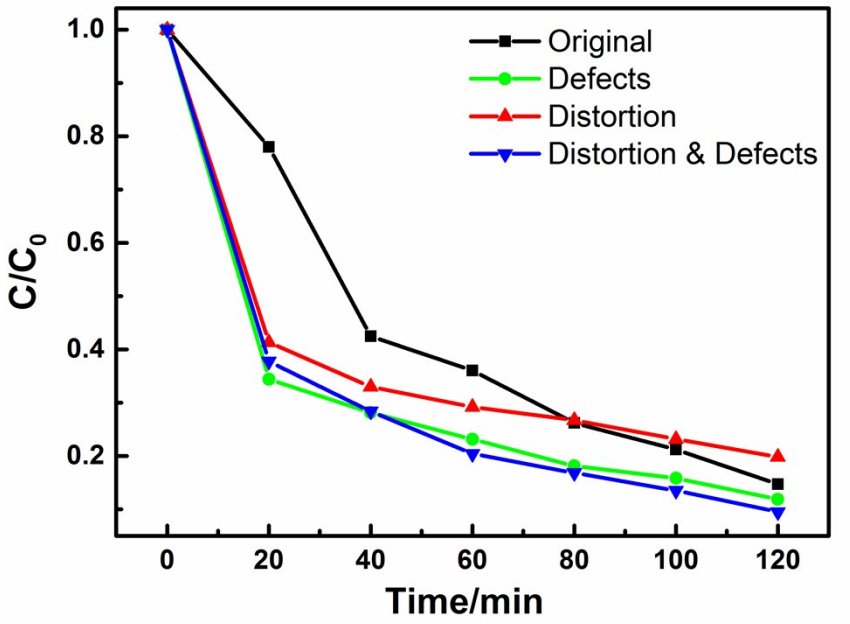

Figure S8. The degradation of phenol using the different TiO_2 samples under visible light irradiation. The degradation tendency of phenol is almost the same as the degradation of RhB; therefore, the dye sensitization was not found to be that significant.

Table S1. BET Surface area of as-prepared TiO_2 samples

Sample	Original	Distortion	Defects	Distortion & Defects
Surface area (m^2/g)	185	188	114	143

Theoretical Calculation

Density functional theory (DFT) calculations are carried out with a VASP package (the Vienna *ab initio* Simulation Package) using plane wave basis sets with a cutoff of 340 eV. The generalized gradient approximation with the function of Perdew-Burke-Ernzerhof (PBE) is utilized for all geometric optimization and energy calculation. A 2×2×1 supercell containing 24 Titanium atoms and 48 Oxygen atoms was employed, where a vacuum of 10 Å is used to simulate the surface in periodic boundary condition. The effect of chlorine is simulated by adding 4 Chlorine atoms above the (101) surface of TiO_2 within vacuum layer. The bond length change was calculated through geometry optimization and the energy change was calculated through energy calculations.

It was found that the length of the Ti-O bond increases from 1.780 Å to 1.802 Å with the existence of Cl atoms due to its higher electronegativity than O ion, resulting in the lattice expanding on the surface of TiO_2. Surface oxygen ions in these distorted TiO_2 lattices are easier to be removed and oxygen vacancies are easier to be generated on the basis that less energy (~0.032 eV less) are required in lattice-distorted areas (6.08 eV) than in perfect lattice areas (6.11 eV).